

PAPER

Concentric-ring-grating-induced strong terahertz near-field enhancement on a micro-tip

To cite this article: Xinfeng Zhou *et al* 2019 *J. Opt.* **21** 105005

View the [article online](#) for updates and enhancements.



IOP | ebooks™

Bringing you innovative digital publishing with leading voices to create your essential collection of books in STEM research.

Start exploring the collection - download the first chapter of every title for free.

Concentric-ring-grating-induced strong terahertz near-field enhancement on a micro-tip

Xinfeng Zhou¹, Xuguang Guo^{1,4} , Alexander Shkurinov^{2,3} and Yiming Zhu¹

¹ School of Optical-Electrical and Computer Engineering, Shanghai Cooperation Innovation Centre of Terahertz Spectroscopy and Imaging Technology, Shanghai Key Lab of Modern Optical System and Engineering Research Center of Optical Instrument and System, Ministry of Education, University of Shanghai for Science and Technology, 516 Jungong Road, Shanghai 200093, People's Republic of China

² Department of Physics and International Laser Center, M. V. Lomonosov Moscow State University, 1 Leninskie Gory, Moscow 119992, Russia

³ ILIT RAS – Branch of FSRC ‘Crystallography and Photonics’ RAS, Shatura 140700, Russia

E-mail: xgguo_sh@qq.com

Received 18 March 2019, revised 8 August 2019

Accepted for publication 21 August 2019

Published 20 September 2019



CrossMark

Abstract

A terahertz near-field source, composed of a subwavelength metallic concentric ring grating on a dielectric slab with a micro-tip, is proposed. The field enhancement property and the field distribution near the tip apex are studied theoretically. A volume-averaged energy density enhancement factor of 550 around the tip apex region could be obtained for radial polarized field illumination. Compared with conventional scanning near-field optical microscopies (SNOMs), about 15-fold enhancement of near-field energy density is obtained by using the proposed near-field source. We attribute such a strong enhancement to the guided resonant modes launched by the radial grating, the axial symmetry of the device, and the radial polarization of incident beam. The resonance frequencies of the device are controlled by varying the grating period and the thickness of dielectric substrate. The proposed device is useful for improving the coupling efficiency of SNOMs.

Keywords: nano focusing, guided resonance mode, near-field enhancement, sub-wavelength imaging

(Some figures may appear in colour only in the online journal)

Terahertz technology has been widely applied to noninvasive imaging, spectroscopy, biomedical and semiconductor quality control, and security technologies [1, 2] due to the low terahertz photon energy (~ 4 meV at 1 THz). However, the Abbe diffraction limit restricts the spatial resolution of far-field imaging techniques. Scanning near-field optical microscopy (SNOM) has drawn increased attention in past decades, since it offers the possibility to realize deep subwavelength spatial resolution. SNOMs usually go beyond the Abbe diffraction limit by using a subwavelength aperture [3–6] based on the principle proposed by Syngé in 1928 [7] or using a micro tip probe (scattering SNOMs, s-SNOMs) [8–10]. Furthermore, it was demonstrated

that s-SNOMs are capable of providing better spatial resolution and coupling efficiency. Moreover, the s-SNOM technology is much more flexible and compatible to integrate to conventional optical systems and can also be applied to nanoscale manipulating applications at infrared and visible frequencies [11–13].

While the development of s-SNOM technology at infrared and visible frequencies has rapidly advanced in the last century, terahertz s-SNOM technology is relatively new and has only seen significant progress in the last three decades [14–16]. Nevertheless, the wide range of possible applications of today's terahertz near-field technology is stimulating enormous attention from various fields. Especially for semiconductor quality control and basic property research, a lot of works on both terahertz near-field technology and applications have been

⁴ Author to whom any correspondence should be addressed.

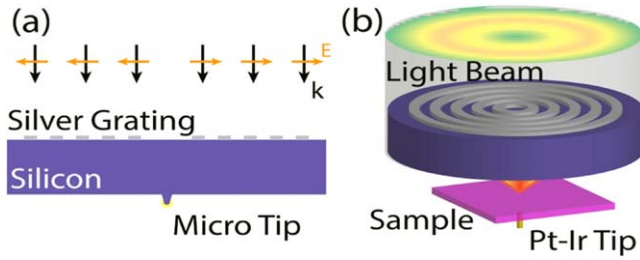


Figure 1. (a) The device with 1 μm thick silver radial grating on the 200 μm thick silicon substrate with a tip on the other side and (b) proposed setup in an s-SNOM with a cascade focus scheme.

reported recent years [17–24]. Terahertz s-SNOM has been a unique technology to determine the properties of semiconductors and biomedical materials [24]. The micro-tip of an s-SNOM brings deep subwavelength spatial resolution, near-field enhancement and more flexible applications with different novel configurations. However, due to the mismatch between the relative long wavelength of terahertz wave ($\sim 100 \mu\text{m}$) and the tiny tip apex size ($\sim 20 \text{ nm}$), the light coupling efficiency at terahertz range is ultralow, at a level of 10^{-4} [25]. Thus, it restricts the imaging performance and demands high power illumination sources. Since the terahertz near-field technology is much younger than other ones, there are few works on coupling efficiency and high efficient near-field sources [25–29]. The ultralow coupling efficiency from far-field to near-field obstructs industrial application progress in the terahertz range.

To realize both the high spatial resolution and high scattering efficiency, we propose a device composed of a concentric ring metallic grating on one side of a dielectric slab and a micro-tip mounted on the other side of the slab (figure 1). It can be used as the first stage in a cascade focus scheme providing a novel illumination method for s-SNOMs to improve the coupling efficiency and bring strong tip-sample interaction. Theoretical calculations and numerical simulations are performed to explore the local field enhancement under illuminations with linear- and radial-polarized light beams. The terahertz field with radial polarization impinging on the device can be focused near the micro tip in a deep subwavelength scale of several μm volume and with a strong volume-averaged energy density enhancement factor of 550 defined by the ratio of the energy around the tip apex region with and without the grating coupler. The strong local field enhancement is introduced by the guided resonant modes [30] in the grating-dielectric-slab structure [31]. The guided resonant frequencies are determined theoretically by solving the eigenvalue equation of the planar dielectric (Si) slab waveguide. Numerical simulations show the similar guided resonance properties for the slab waveguides with straight and concentric ring gratings, illuminated with TM and radially-polarized beams, respectively. Because of the total reflection for the guided resonant modes at the bottom surface of the device, the radial polarization of incident beam [32–35], and the axisymmetric geometry, the field confined at the apex is totally longitudinally polarized under illumination of radial-polarized light [36], which is useful for manipulating the tunnel probability of carriers or accelerating particles. In

comparison with conventional s-SNOMs, the numerical results show that about 15-fold enhancement of near-field energy density can be obtained by using the proposed device.

The proposed device consists of a concentric ring silver grating with period of 300 μm , duty cycle of 50%, and strip height of 1 μm . The inner radius of the smallest ring is 300 μm . The high-resistivity silicon substrate is 200 μm thick. In the center of the circular substrate, there is a 2 μm high silicon micro-tip with a 1- μm apex radius on the other side of the gratings. The commercial software, COMSOL (version 5.2a), is used to compute the reflectance and field distribution. The relative dielectric constant of silver is described by the Drude model,

$$\varepsilon(\omega) = 1 - \frac{\omega_p^2}{\omega^2 + i\gamma\omega}. \quad (1)$$

The parameters used in the Drude model for silver are plasma frequency $\omega_p = 1.37 \times 10^{16} \text{ rad s}^{-1}$ and collision frequency $\gamma = 7.29 \times 10^{13} \text{ rad s}^{-1}$ [37]. When using the above parameters, the imaginary part can be omitted, because silver can be treated as PEC at the terahertz frequency domain. Then, equation (1) can be written as $\varepsilon(\omega) = 1 - \omega_p^2/\omega^2$. The refractive index of silicon is 3.5 given as a constant. Due to rotational symmetry of both the illumination source and the device structure, numerical simulations can be performed using a 2D axisymmetric model template integrated in COMSOL. Also, we use an interior port as the illumination source. The formula of the radially-polarized source is defined as

$$E_{rp}(r) = r \times \exp\left[-\left(\frac{r}{w}\right)^2\right], \quad (2)$$

where r represents the distance to the symmetric axis, and the value of w is 1.5 mm as the beam waist.

The field enhancement mechanism of the device can be qualitatively described as follows. The concentric-ring grating is a coupler, through which the guided modes supported by the Si slab can be excited by a normal incident beam with radial polarization at the resonant frequencies determined by the dispersion relations of the guided modes and the periodicity of the grating (figure 2(a)). At these resonant frequencies, the field energy is effectively funneled into the slab and the resonant waveguide modes with low group velocities are launched, and due to the total reflection at the slab surface opposite to the concentric ring grating, strong evanescent fields bounded to the surface are excited. Because of the circular symmetry of the device and the radial polarization of the incident beam, large evanescent field enhancement near the tip apex is expected.

The resonant frequencies are theoretically evaluated with three steps. First, we assume that the reflection spectra and the resonant behaviors are similar for the two configurations of straight grating under illumination of TM waves (electric field across the grating strips) and the concentric ring grating under illumination of radially polarized waves. Such an assumption is verified by numerical simulations (figure 2(b)). Second, the guided mode dispersion relations of the planar slab $\omega(\beta)$ are determined by solving the transcendental equation (equation (3))

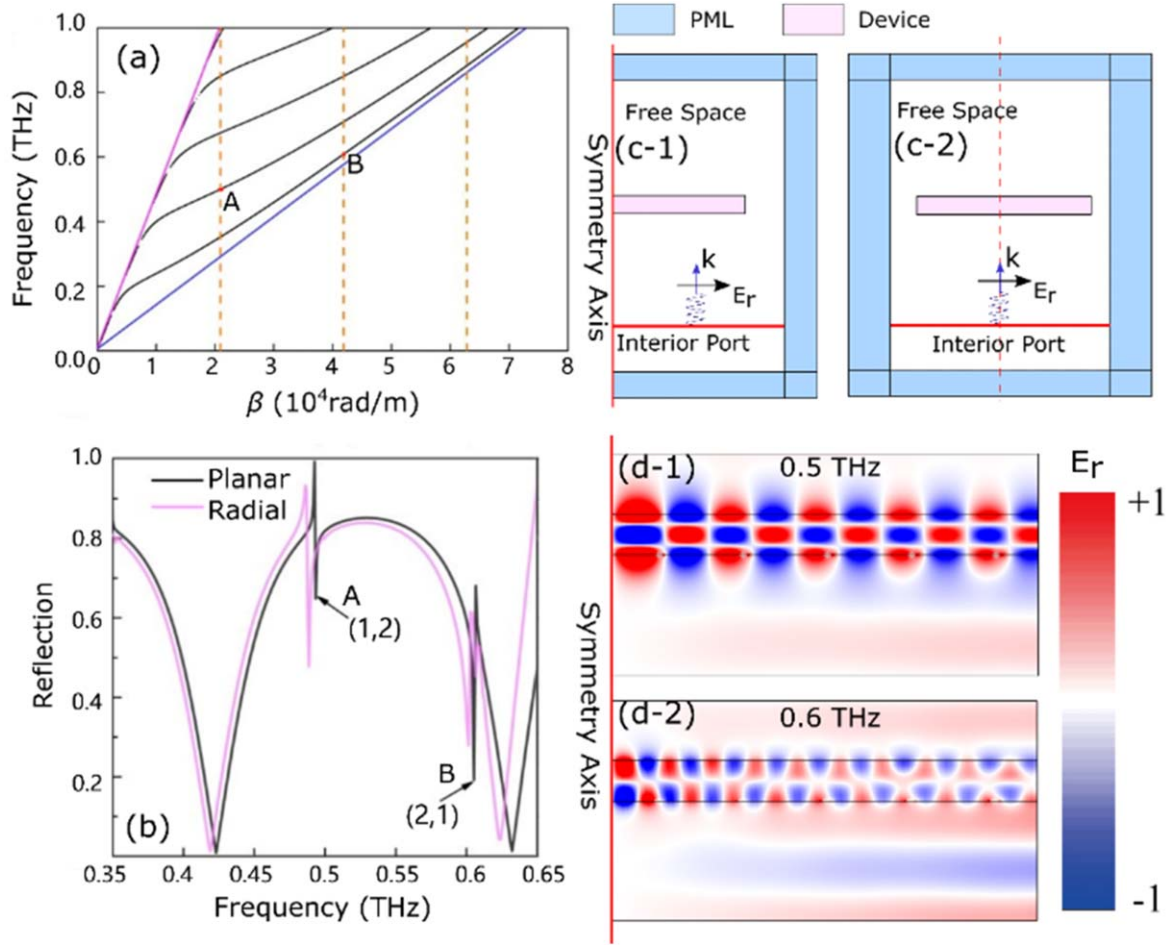


Figure 2. (a) Dispersion relations of the slab waveguide modes. The black lines represent dispersion relations of the silicon slab waveguide modes; the purple line and blue line represent the dispersion relations in the silicon and vacuum, respectively; the orange dashed lines represent the matched wave vector given by the metallic grating for resonance frequencies. Points A and B show the guided mode resonances (1,2) and (2,1) at ~ 0.5 THz and ~ 0.6 THz, respectively. (b) A comparison of the numerical reflection spectra of the straight grating illuminated by a TM beam and the concentric ring grating illuminated by a radial-polarized beam. (c) The computational configuration schemes for radial gratings and straight gratings are shown in (c-1) and (c-2), respectively. (d) E_r components of electric field at guided mode resonance frequencies marked by A (d-1) and B (d-2).

with the given slab thickness d and refractive index n .

$$\begin{aligned} \tan \kappa d &= n_1^2 \kappa^2 (n_3^2 \gamma + n_2^2 \delta) / (n_2^2 n_3^2 \kappa^2 - n_1^4 \gamma \delta) \\ \kappa &= (n_1^2 k^2 - \beta^2)^{\frac{1}{2}} \\ \gamma &= (\beta^2 - n_2^2 k^2)^{\frac{1}{2}} \\ \delta &= (\beta^2 - n_3^2 k^2)^{\frac{1}{2}} \end{aligned} \quad (3)$$

where k , β , n_1 , n_2 and n_3 represent wave vector, propagation constant, and refractive indexes of the Si slab, the upper and lower regions of the Si slab waveguide, respectively. Third, the guided mode resonance frequencies are obtained at the wave vector values of $\beta = 2\pi m/p$ with m and p being an integer and the periodicity of the grating, respectively. Since the metallic grating will introduce an additional phase shifting at the reflection interface, we chose a low grating duty cycle to diminish the additional phase. Here, a low grating duty cycle of 10% is given to perform the numerical simulation for both the straight and the concentric ring gratings. We find that both of their resonant frequencies match well with the theory. Both the Fano line type

signatures in figure 2(b) and the electric field distributions in figure 2(d) confirm that the strong field enhancement originates from the guided resonances and the resonant frequencies are tunable by varying the thickness of the slab waveguide and the periodicity of the grating [30, 38].

The hybrid grating-dielectric-waveguide structure can support the guided resonant modes, which can be used to squeeze electromagnetic wave from free space into the waveguide [39]. The reflectance coefficients and field distributions for the structures with and without gratings are simulated. The results (figure 3(a)) indicate that the gratings play an important role in the reflection spectra and the near-field enhancement near the micro-tip. The dashed line in figure 3 demonstrates the reflection spectrum of Fabry-Pérot (FP) resonance of the planar silicon dielectric slab without grating. The dashed-dotted line shows the situation with the grating. There are many grating-introduced new features in the reflection spectrum, and these new features are due to the excitation of guided resonant modes in the silicon slab, which results in the field enhancement in the dielectric slab. The guided resonant modes satisfy

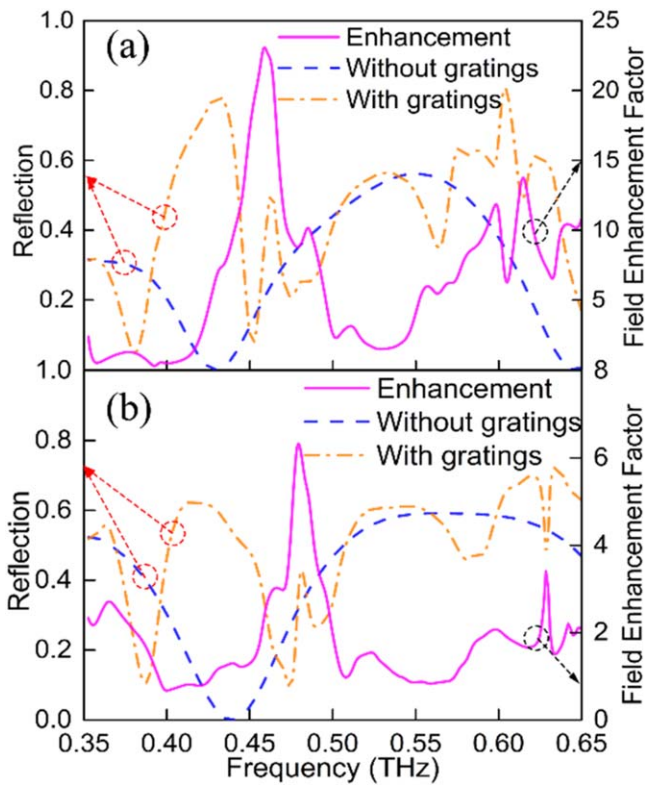


Figure 3. The reflection spectra and field enhancement factors of device with radial grating illuminated by a radial-polarized beam (a) and the device with straight grating under illumination of linear polarization source (b).

the total reflectance condition on the other surface of the dielectric slab. Hence, it is expected that there are enhanced evanescent fields near the surface and the micro-tip at the resonant frequencies. The enhancement factor is defined as the ratio of the volume-averaged field intensity $|E|^2$ near the micro-tip apex with and without grating. As depicted in figure 3(a), a very strong near-field enhancement can be achieved at 0.46 THz and 0.61 THz. The corresponding energy density enhancement factors of 550 and 200 can be achieved. To confirm the contributions of axisymmetric geometry and the radially polarized source, we compare the results for straight and concentric ring gratings with the same parameters stimulated by linearly and radially polarized beams, respectively. In order to match the setup of concentric ring grating, there is a strip absent at the center of the device with the straight grating. For a linearly polarized input field, guided resonances and field enhancement can be achieved at 0.48 THz and 0.63 THz as well, and the corresponding energy density enhancement factor of 40 and 14 can be achieved with linear polarization source. It is obvious that the symmetric property of radially polarized beam and the concentric ring grating contribute remarkably to strong near-field enhancement near the micro tip. At the resonant frequencies, the local field enhancement factors reach their maximum values, and Fano line shape signatures exist in the reflectance spectra, which identifies that the near-field enhancement originates from the guided resonant modes and the spatial constructive interference of fields from the 2π angular space.

The field at the tip apex is shown in figure 4. The field is tightly confined to the tip apex. In comparison with the background field, it can be concluded that the field confined to the apex is an evanescent field and it cannot propagate in the free space. As shown in figure 4(a), most field energy is confined to the apex, and decreases sharply along the z axis at a length of $1.0 \mu\text{m}$, which confirms that the field is an evanescent one. The field intensity at the cutline of $z = 2.1 \mu\text{m}$ shows the full width at half maximum (FWHM) of field intensity is about $2.0 \mu\text{m}$. The largest enhancement factor of 550 near the micro-tip apex is reached at 0.46 THz for the proposed device illuminated by a radial polarized light beam. The polarization properties for the two cases are shown in figures 4(b) and (c), which indicates that the near-field polarization is related to the polarization of the incident wave. This near-field at the tip region can be measured experimentally through the full vectorial terahertz near-field mapping technology [40]. As shown in figure 4(c), the field near the apex only has a z component under radial-polarized light for the symmetric properties of both the incident wave and the proposed device. It can help the electron to overcome the barrier and reach the STM tip. As a result, the longitudinal field will improve the sensitivity of photon-assisted tunneling detection in s-SNOMs based on scanning tunneling microscopy. It also can lower the bias voltage to manipulate particles with the STM tip [41, 42].

From the numerical results, we can conclude that the guided resonant modes, total reflection, and evanescent wave interference at the tip apex are responsible for the strong local field enhancement. First, the frequency of incident light should fulfill the excitation condition of guided resonant modes, which is determined by the parameters of grating and the substrate slab. Then the field energy can be effectively funneled into the slab with a minimal reflectance coefficient. The total reflection condition is satisfied at the interface of the proposed device, and consequently, bounded evanescent waves exist near the surface. Finally, these evanescent waves must have a constructive interference at the tip apex in the device center. Then we can get a significant energy enhancement factor. From figures 2(a) and 3, we can find the field enhancement factors vary from the order of the guided modes in the dielectric slab. The main enhancement peak and the lower one respectively originate from the first and the second diffraction orders at the resonance frequencies marked by A and B in figures 2(a) and (b).

To compare with conventional s-SNOMs, both the near-field enhancements of proposed device and conventional s-SNOMs are evaluated (figure 5). The near-field enhancement for the proposed device is defined as the ratio of $E_{\text{tip}}/E_{\text{inc}}$, where E_{tip} is the volume-averaged field in a cylindrical region with diameter of $2 \mu\text{m}$ and height of $1 \mu\text{m}$ above the tip apex, and E_{inc} is the area-averaged incident field. It is so difficult to solve the Maxwell's equation after introducing metallic grating and radial polarized light into our model both E_{tip} and E_{inc} are given by the numerical result set. The near-field enhancement reaches 65.67 for the device at 0.46 THz. The near-field enhancement of conventional s-SNOMs is evaluated by considering the gain of the focus

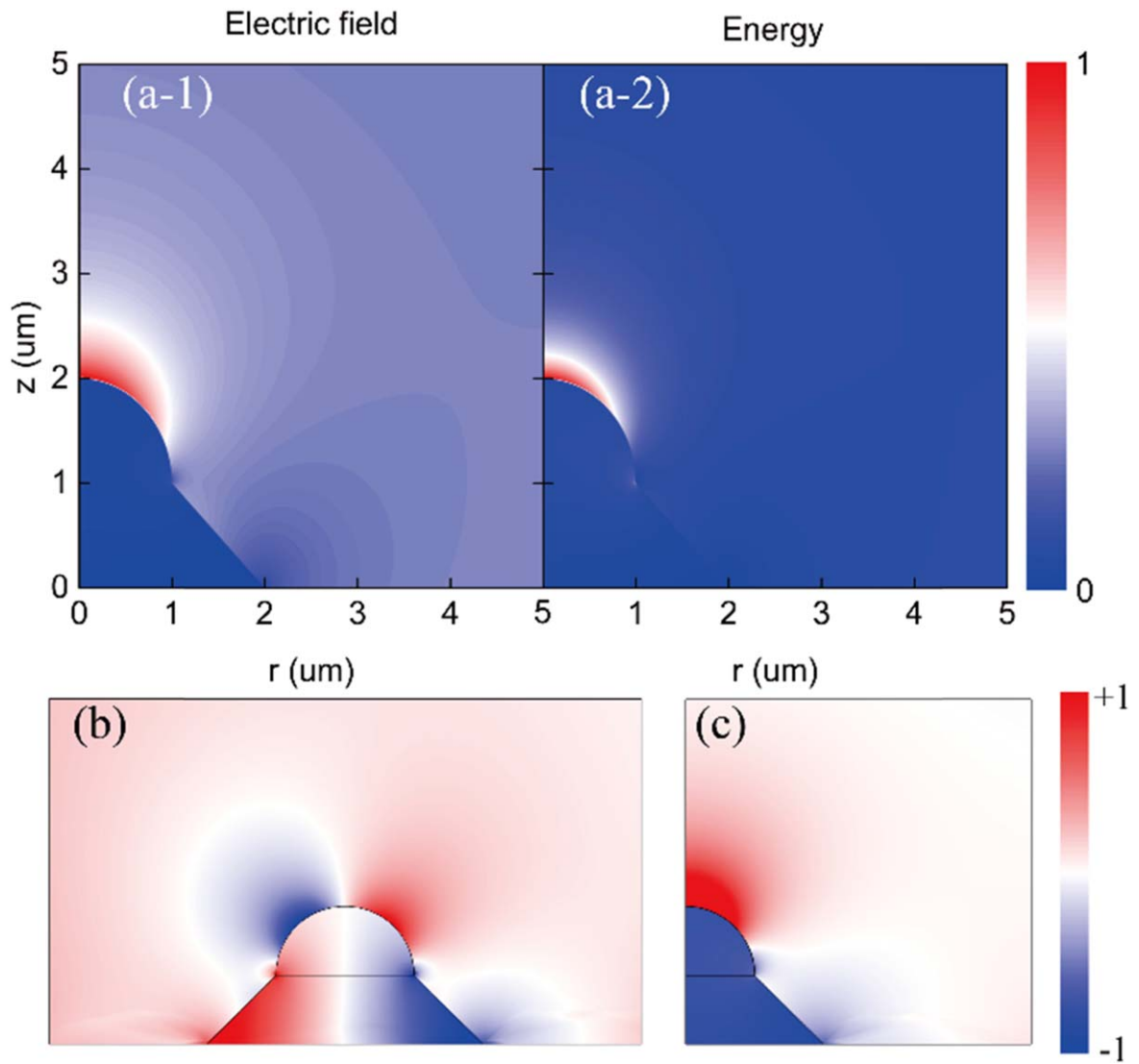


Figure 4. (a) Normalized electric field intensity and energy density distribution around the micro-tip apex for a radially polarized input field, (b) z component of electric field distribution at the tip apex of straight grating for linearly polarized input field, and (c) the case of concentric ring gratings for radially polarized input field.

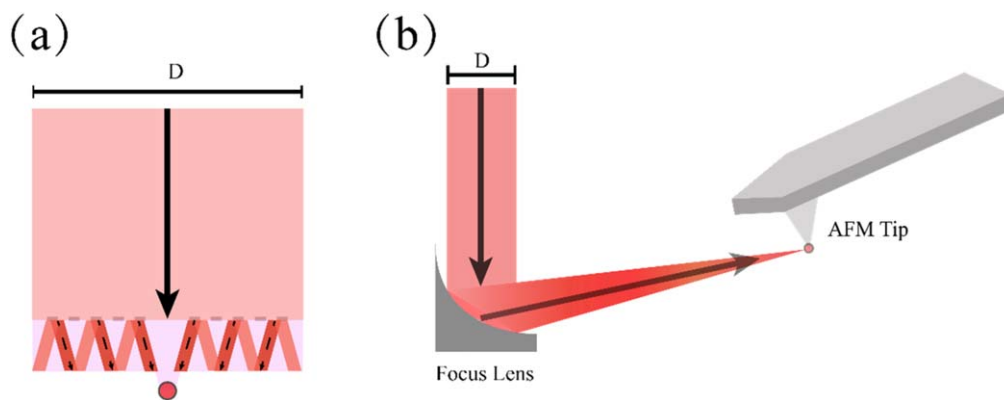


Figure 5. (a) The direct cascade focusing scheme for the proposed device and (b) conventional focus scheme for s-SNOMs. Both the incident field with a diameter of $D = 3.3$ mm, share the width with the proposed device.

lens theoretically (an off-axis parabolic mirror with the NA of 0.4) and the dipolar resonant effect (figure 5(b)). We assume the THz beam (beam diameter of 3.3 mm, the diameter of the proposed device) can be focused to a spot with the diameter limited by diffraction. For an AFM tip, the dipolar near-field enhancement factor is about 10 [43]. Then, the near-field enhancement for a s-SNOM is 16.59 at 0.46 THz. Therefore, the proposed device provides a 15.6-fold enhancement of near-field energy density than the s-SNOMs.

In conclusion, we proposed a tip enhanced structure using guided resonances constructive interference as the first stage of the cascade focus scheme for s-SNOMs. The radial grating introduces spectral features by exciting guided resonant modes [31]. The tip enhancement effect surpasses the diffraction limitation to a spatial resolution approximating $\lambda/300$ in the terahertz regime, provides a point-like near-field source illuminating the samples. The evanescent field constructive interference at the tip apex gives a significant energy density enhancement factor of 550 and provides 15.6 times enhancement of near-field energy density than conventional s-SNOMs. In addition, the device will not introduce any background scattering or reflection. Thus, it eliminates the background field noise and improves the imaging contrast. The totally longitudinal field at tip apex under illumination with radial polarized beam is useful for light-assisted tunneling current amplification.

Acknowledgments

This work was supported in part by the National Natural Science Foundation of China (61731020, 61722111), the National Key Research and Development Program of China (2017YFA0701005), the 111 Project (D18014), the International Joint Lab Program supported by Science and Technology Commission Shanghai Municipality (17590750300), and the Young Yangtse River Scholar (Q2016212).

ORCID iDs

Xuguang Guo  <https://orcid.org/0000-0003-1733-6478>

References

- [1] Jepsen P U, Cooke D G and Koch M 2011 *Laser Photon. Rev.* **5** 124
- [2] Hafez H A, Chai X, Ibrahim A, Mondal S, Férachou D, Ropagnol X and Ozaki T 2016 *J. Opt.* **18** 093004
- [3] Ash E and Nicholls G 1972 *Nature* **237** 510
- [4] Pohl D W, Denk W and Lanz M 1984 *Appl. Phys. Lett.* **44** 651
- [5] Dürig U, Pohl D W and Rohner F 1986 *J. Appl. Phys.* **59** 3318
- [6] Betzig E, Trautman J, Harris T, Weiner J and Kostelak R 1991 *Science* **251** 1468
- [7] Sygne E 1928 *Phil. Mag.* **6** 356
- [8] Zenhausern F, Martin Y and Wickramasinghe H 1995 *Science* **269** 1083
- [9] Knoll B and Keilmann F 2000 *Opt. Commun.* **182** 321
- [10] Frey H G, Witt S, Felderer K and Guckenberger R 2004 *Phys. Rev. Lett.* **93** 200801
- [11] Sheng S, Wu J-B, Cong X, Li W, Gou J, Zhong Q, Cheng P, Tan P-H, Chen L and Wu K 2017 *Phys. Rev. Lett.* **119** 196803
- [12] Keyi W, Zhen J and Wenhao H 1998 *Opt. Commun.* **149** 38
- [13] Kühn S and Sandoghdar V 2006 *Appl. Phys. B* **84** 211
- [14] Amarie S, Ganz T and Keilmann F 2009 *Opt. Express* **17** 21794
- [15] Wächter M, Nagel M and Kurz H 2009 *Appl. Phys. Lett.* **95** 041112
- [16] Cho G C, Chen H T, Kraatz S, Karpowicz N and Kersting R 2005 *Semicond. Sci. Technol.* **20** S286
- [17] Hunsche S, Koch M, Brener I and Nuss M C 1998 *Opt. Commun.* **150** 22
- [18] Lecaque R, Grésillon S, Barbey N, Peretti R, Rivoal J C and Boccara C 2006 *Opt. Commun.* **262** 125
- [19] Bitzer A and Walther M 2008 *Appl. Phys. Lett.* **92** 231101
- [20] Adam A J, Brok J M, Planken P C, Seo M A and Kim D S 2008 *C. R. Phys.* **9** 161
- [21] Huber A J, Keilmann F, Wittborn J, Aizpurua J and Hillenbrand R 2008 *Nano Lett.* **8** 3766
- [22] Blanchard F, Doi A, Tanaka T, Hirori H, Tanaka H, Kadoya Y and Tanaka K 2011 *Opt. Express* **19** 8277
- [23] Cocker T L, Jelic V, Gupta M, Molesky S J, Burgess J A, De Los Reyes G, Lyubov V T, Ying Y T, Mark R F and Hegmann F A 2013 *Nat. Photon.* **7** 620
- [24] Chen L, Liao D, Guo X, Zhao J, Zhu Y and Zhuang S 2019 *Front. Inf. Technol. Electron. Eng.* **20** 591
- [25] Chen L, Wei Y, Zang X, Zhu Y and Zhuang S 2016 *Sci. Rep.* **6** 22027
- [26] Sqalli O, Bernal M-P, Hoffmann P and Marquis-Weible F 2000 *Appl. Phys. Lett.* **76** 2134
- [27] Brehm M, Schliesser A, Čajko F, Tsukerman I and Keilmann F 2008 *Opt. Express* **16** 11203
- [28] Rui G, Chen W, Lu Y, Wang P, Ming H and Zhan Q 2010 *J. Opt.* **12** 035004
- [29] Wang K, Mittleman D M, Valk N C and Planken P C 2004 *Appl. Phys. Lett.* **85** 2715
- [30] Fan S and Joannopoulos J D 2002 *Phys. Rev. B* **65** 235112
- [31] Li J, White T P, O'Faolain L, Gomez-Iglesias A and Krauss T F 2008 *Opt. Express* **16** 6227
- [32] Oron R, Blit S, Davidson N, Friesem A A, Bomzon Z and Hasman E 2000 *Appl. Phys. Lett.* **77** 3322
- [33] Wróbel P, Pniewski J, Antosiewicz T J and Szoplík T 2009 *Phys. Rev. Lett.* **102** 183902
- [34] Winnerl S, Zimmermann B, Peter F, Schneider H and Helm M 2009 *Opt. Express* **17** 1571
- [35] Dorn R, Quabis S and Leuchs G 2003 *Phys. Rev. Lett.* **91** 233901
- [36] Wang H, Shi L, Lukyanchuk B, Sheppard C and Chong C T 2008 *Nat. Photonics* **2** 501
- [37] Shin H, Catrysse P B and Fan S 2005 *Phys. Rev. B* **72** 085436
- [38] Bezu E A, Doskolovich L L and Kazanskiy N L 2011 *Microelectron. Eng.* **88** 170
- [39] Mizutani A, Kikuta H and Iwata K 2003 *Opt. Rev.* **10** 13
- [40] Bhattacharya A and Rivas J G 2016 *APL Photonics* **1** 086103
- [41] Lyo I-W and Avouris P 1991 *Science* **253** 173
- [42] Stollenwerk A J, Hurley N, Beck B, Spurgeon K, Kidd T E and Gu G 2015 *Phys. Rev. B* **91** 125425
- [43] Esteban R, Vogelgesang R and Kern K 2005 *Nanotechnology* **17** 475